Critical Review of the Root Cause Investigation of Crystal River Delamination

December 2019

BY

Victor E. Saouma

University of Colorado, Boulder

X-Elastica, LLC

Contents

List of Figures

List of Tables

1 Introduction

Inside nuclear reactors, the release of high-energy neutrons causes long-term degradation of material, including neutron embrittlement which will result in reduced toughness and cracking (Chopra, 2015). When this becomes unmanageable, then replacement of units must be undertaken. This is indeed a major problem for the massive heat exchange units (also known as steam generator) that may have to be replaced to ensure safe (crack free) continuous operation of the plant (Booker et al., 1994).

Progress Energy had to replace the heat exchanger in Crystal River 3. Given the size, it had to cut a 27-by-27-foot hole in the 187-foot-tall containment enclosure building (CEB) to extract the unit. However, since the CEB was post-tensioned, cables had to be judiciously detentioned. A task successfully accomplished in other sites. However, it this case Progress Energy opted to self manage the operation despite internal studies warning it of "huge" risk Tampa Bay Times (2014).

Initially, 97 tendons wee to be detensioned (per calculations by Sargent & Lundy). Given the high cost, Progress reduced the number to 65 that was considered "adequate" by Bechtel. Even then, Progress Energy decided to loosen a total of just 27 tendons. And it hired a company to cut into the nuclear containment wall that had never done that work.

After detensioning, and during concrete removal it was found that the CEB had delaminated. There was an initial attempt to repair the CEB by fully detensioning it[1]. However, this only aggravated the problem, additional delamination occured. Ultimately this operation resulted in extensive cracking that made any further repair impractical, and CR-3 had to be decommissioned (NuclearEnergy Insider, 2019) at a cost of approximately $ 700 millions by 2027.

Hence, an attempt to save $15 million resulted in a $ 3 million loss.

Gregory Jaczko, a past chairman of the U.S. Nuclear Regulatory Commission, blamed the disaster on a utility that didn't understand a job that should have been "routine". "That's a multibillion dollar asset that had to be shut down because of improper work planning, improper understanding of how to properly do this containment retrofit".

Most shocking, yet not to the surprise of the author, the Nuclear Regulatory Commission stated that "Analysis has shown that the 2009 delamination (cracking) could not have been predicted" (Progress Energy Florida, 2011).

Ironically, this is not the only shut-down of a nuclear reactor due to problems associated with steam generator replacement (Los Angeles Times, 2013) (a $2 billion loss incurred by the decommissioning's of San Onofre nuclear power plant).

Given the international attention that this accident has generated, and taking advantage of the wealth of publicly available documentation provided by the NRC (which should be commended for its transparency) through "NRC-ADAMS" (2018), this report is an attempt to cast a critical light on the root cause investigation[2]

Hence, this document is composed of three parts. First, relying on publicly available documents, the root cause investigation of Crystal River 3 (CR) will be described in great details. In the second part, the author reviews the finite element analysis, and finally provide an alternate solution.

2 Reported Analyses/Investigation

This section will review (ADAMS Accession No. ML 102861026, 2010) and (Progress Energy Florida (ML102861026), 2009) that is the non-proprietary version of the root cause investigation of the unanticipated delamination of Crystal River Unit 3.

[1] **Disclaimer:** The author was retained by Structural Integrity Associates to be one of the reviewers of the MPR calculations for the detensioning sequence.

[2] **Disclaimer:** The first author was retained as a consultant to PII for the root cause investigation. As such he was privy to some confidential information. None of them will be reported directly or indirectly here. Furthermore, the author did perform a fracture mechanics based analysis of CR-3 that was not retained by PII, and at his request his name was not included in the final report. The author was subsequently retained as consultant by Structural Integrity Associates, Inc. to provide technical support for third party review of CR-3 containment detensioning evaluation and related documents. Again, the confidentiality of those documents is fully respected.

In a pressurized water reactor plant there are three main barriers that protect the public from the radiation hazards associated with nuclear operations, Fig. 1(a). One of those barriers is known as the containment, which houses the fuel, the reactor, and the reactor cooling system. The Crystal River containment structure is a steel lined post-tensioned cylindrical concrete structure of about 157 feet in height with an outside diameter of about 138 feet. The containment has 42- inch thick concrete walls and has a flat foundation mat and a shallow torispherical dome. Posttensioning is achieved by utilizing an outer array of horizontal tendons immediately adjacent to an inner array of vertical tendons that are embedded in the walls about 15 inches from the outside surface (*Study of Post tensioning Methods* 2015). Tendons are also provided in the dome. In addition, steel rebar is embedded in the concrete walls at the outside surface and at other locations.

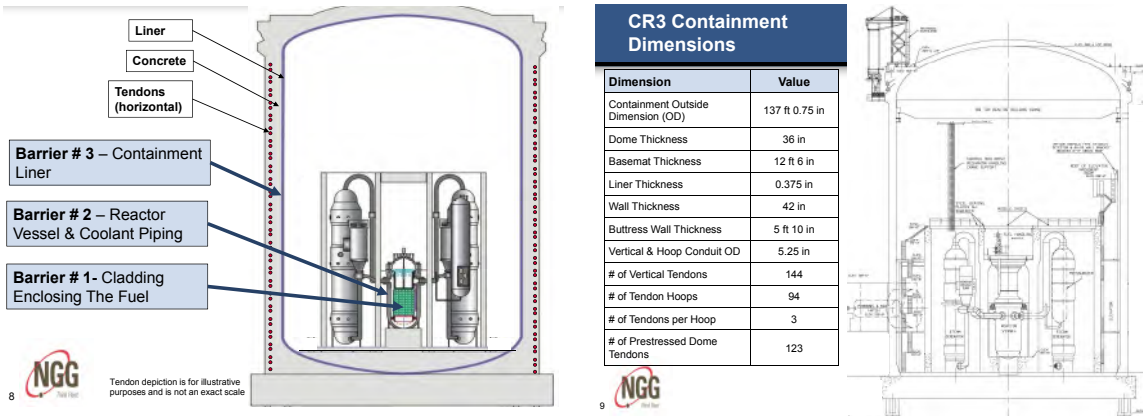

(a) Fission product barriers (b) Crystal River Unit 3 Dimensions

Figure 1: Crystal River Unit 3 characteristics (Progress Energy Florida (ML102861026), 2009)

The containment is lined with a continuous 3/8-inch-thick carbon steel liner (that acts as a vapor barrier for leak-tightness and also as an inner form for the concrete. The dome is post-tensioned by 123 tendons that are arranged in a three-way (layer) configuration and are anchored to a ring girder. The containment walls include 282 horizontal (Fig. 2(a)) and 144 vertical (Fig. 2(c)).

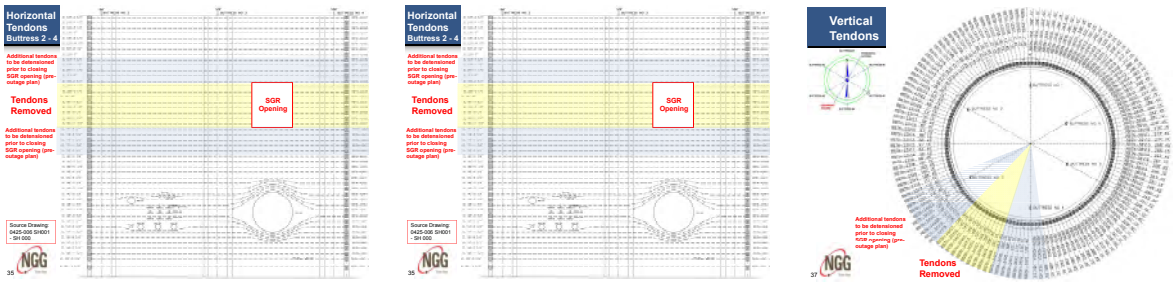

(a) Horizontal tendons, Buttress 2-4 (b) Horizontal tendons, Buttress 3-6 (c) Vertical tendons

Figure 2: Posttensioning cables (Progress Energy Florida (ML102861026), 2009)

Tendons that are anchored to 6 vertical buttresses equally spaced circumferentially around the containment (Fig. 3 and were designed to cross one buttress between the end anchor ones (for the opening, tendons in 2-4 and 3-5 were released). Each tendon consists of numerous small diameter wires, which are greased and housed inside a conduit. The conduit for each tendon is about five inches in diameter and is made of galvanized steel, Fig. 4. The

In nuclear power plants, and in Crystal River in particular, steam generator tubes are commonly fabricated from plain carbon steels, as well as low and high alloy steels.; these components often fail catas-

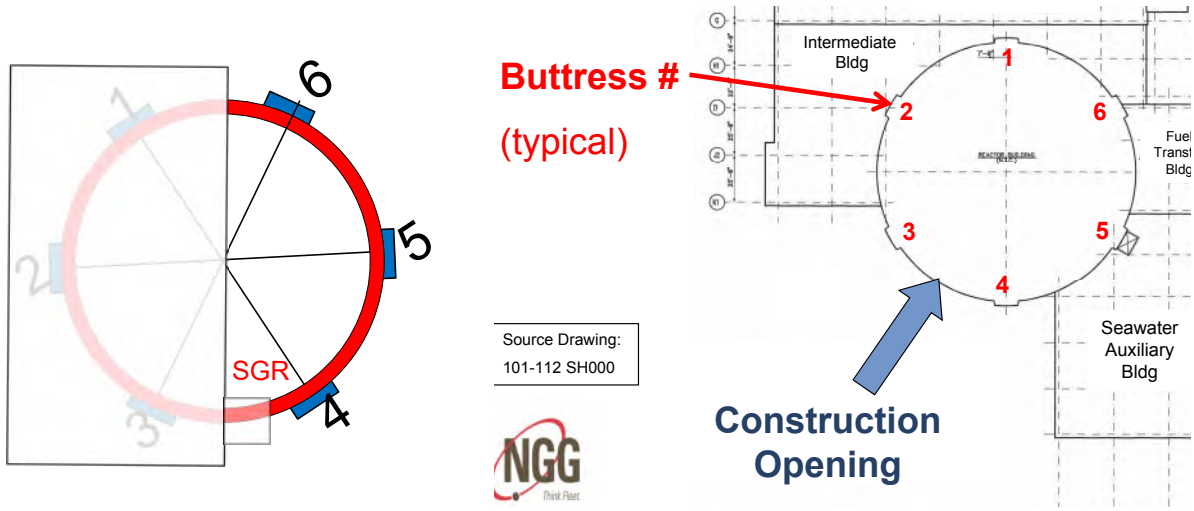

Figure 3: Six anchoring buttresses (Progress Energy Florida (ML102861026), 2009)

Figure 4: 5" tendon conduits (Progress Energy Florida (ML102861026), 2009)

trophically due to hydrogen embrittlement. At some point, continuous repairs may become prohibitively expensive, and the entire unit must be replaced. Though an equipment hatch is present in all containments, it was not large enough for the steam generators to be removed intact or replaced and as an alternative 25' by 27' opening through the 42 inch thick containment unit was envisioned, Fig. 7(d).

Prior to cutting (through hydro-demolition with pressure as high as 25,000 psi) post-tensioned tendons crossing the opening were properly released, Fig. 6(a), then the concrete was "excavated" according to the sequence shown in Fig. 5.

In the process of cutting such an opening in the concrete containment wall a concrete separation condition was discovered, Fig. 7(a). It was located approximately in the cylindrical plane of the centerline of the hoop tendons, approximately nine to twelve inches from the exterior surface of the containment building and had the shape of a butterfly Fig. 6(b).

Approximately 30 inches of concrete remained in apparent good condition all the way to the liner plate. The hydro-demolition of the concrete continued when the containment building liner was exposed and all concrete had been removed down to the liner, Fig. 7(b).

The licensee's investigation concluded that the delamination was caused during the creation of the opening in containment, Fig. 7(c). As part of preparing the containment building for making the opening, tendons

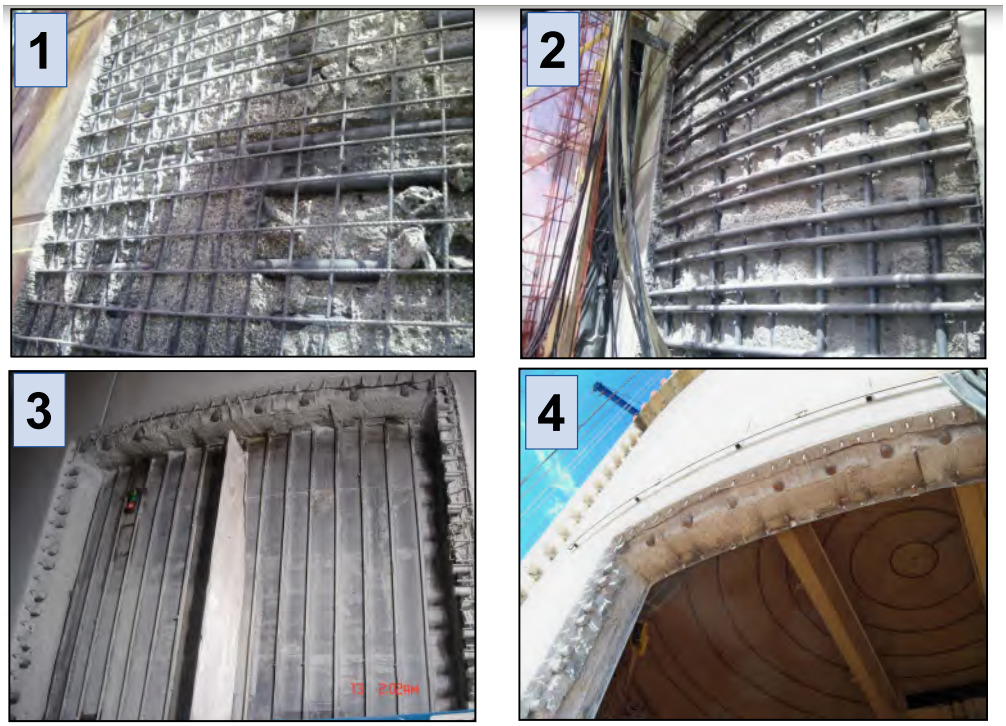

Figure 5: Concrete and liner removal sequence (Progress Energy Florida (ML102861026), 2009)

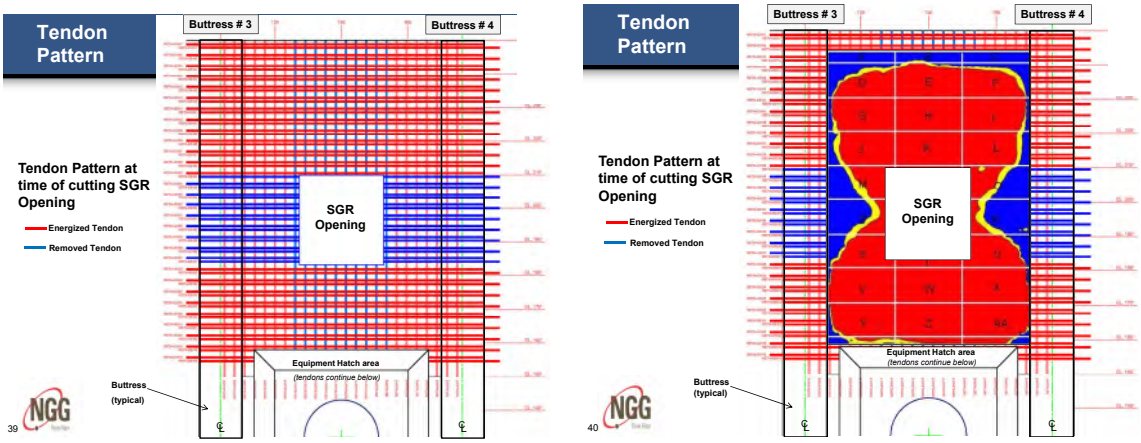

(a) Active and passive tendons

(b) Buterfly defect

Figure 6: Tendon pattern (Progress Energy Florida (ML102861026), 2009)

in the containment building wall were detensioned. The main cause of the delamination was attributed to the scope and sequence of this tendon detensioning. Tendon detensioning began after the plant was shut down in Operating Mode 5, when containment operability was not required.

The licensee found that the delamination was centered on the steam generator opening and formed the shape of an hour-glass. The delamination was limited to the containment bay between buttresses 3 and 4, and did not affect other bays of containment. The licensee's repair plan to remove and replace the delaminated condition included: (1) additional detensioning of containment; (2) removal of delaminated concrete; (3) installation of reinforcement, including radial reinforcement through the delamination plane; (4) placing of new concrete; (5) retensioning containment; and (6) post-repair confirmatory system pressure testing.

(a) Delamination

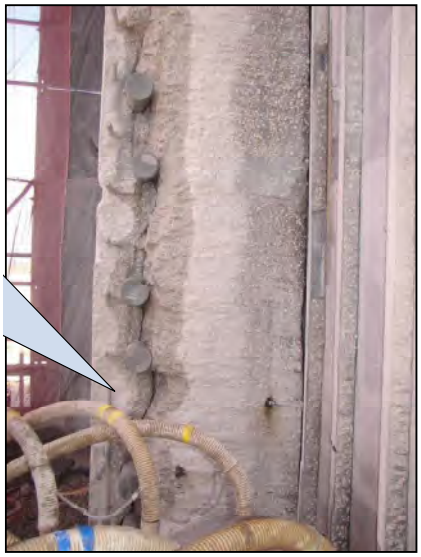

(b) Exposed liner

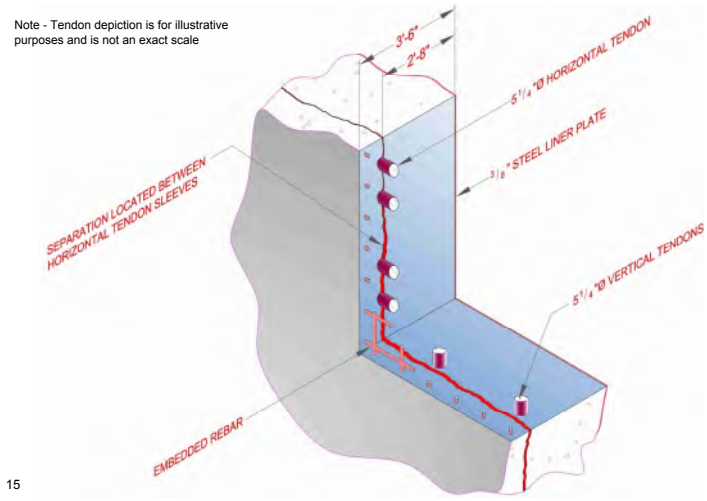

(c) Delamination explained

(d) Steam Generator Replacement opening (between buttresses 3 and 4)

Figure 7: Delamination of Crystal River (Progress Energy Florida (ML102861026), 2009)

The licensee developed new finite element analysis models to predict stresses in the repaired containment wall under design basis loads. Using these and other supporting new analysis models, the licensee planned and implemented additional containment detensioning without causing further delamination. Subsequent to removal of the delaminated concrete, vertical cracks were observed along the vertical tendon lines.

Ultimately, when the cost of fixing the broken containment rose too high, the owner opted to permanently shut down the facility before its original operating license expired.

2.1 Finite Element Modeling

This section will attempt to present four important topics covered in the report in the following sequence:

1. Failure modes associates with Group 1.
2. Failure modes associated with Group 7.

3. Attachment 1 Computer Modeling.
4. Attachment 2 Benchmarking the computer model against plant data.

However for increased clarity, the attachments will be presented first (as they provide explanation/justification for the model used), followed by the two groups.

Computer Model Though not clearly stated PII developed two models

Global Model of the entire Nuclear Containment Structure (NCS). It is a linear elastic model which seeks to capture creep through a visco-elastic model fracture model. It uses th implicit version of Abaqus. This model was used to provide boundary condition displacements to the next more refined model.

Detailed model of a wall panel which encompases 6 horizontal and 3 vertical tendons. Meshing is identical to the global one with two major differences: a) A concrete layer immediatly surrounding the tendon sleeves is modeled by the Lee-Fenves concrete damaged plasticity model (Lee and Fenves, 1998); and b) the explicit version of Abaqus is used.

Back to the report, and quoting from the report, PII recognizes the need to balance mesh refinement with time steps, and seeks a trade-off between accuracy and computational time. Hence PII *created a series of computer codes to simulate the entire building and execute detailed calculations for the particular area of interest. The role that each code part played in the larger framework of the computer model is detailed.* NASTRAN was used for preliminary linear-elastic models to *calculate local conditions and then Abaqus to evaluate the local conditions and determine if damage resulted. However, due to limitations in the model, it was necessary to assume a modulus of elasticity of* 1.1×10^6 *psi throughout the structure. While this assumption allowed the model to predict the onset of delamination it had significant uncertainty.*

PII then used "Abaqus Global" *model using a visco-elastic fracture model and a detailed sub-model for decreased mesh sizing to provide accurate stress predictions. There are four input values which can be adjusted to make the computer model output match the benchmark data, Table 1. Though the Global/Detailed values are redacted (i.e. blackened) they are identified as the two subjected to adjustments to reflect the analysis mesh size used.* Creep coefficient, defined as c in

Parameter	Typical Value	Abaqus Global/Detailed	Impact
Tensile Capacity	500 psi	Redacted	Onset of Cracking
Fracture Energy	0.40 lbf/in	Redacted	onset of Cracking
Elastic Modulus	3.45 $\times10^6$ psi	Redacted	Radial Displacement
Creep Coefficient	2.2	Redacted	Radial Displacement

Table 1: Input Values adjusted for matching

$$E' = \frac{E}{1+c} \tag{1}$$

The couple of c and E' are redacted, implying that they may not be the same as the one shown in Table 1.

PII reports to have reduced *the level of uncertainty by developing a linear elastic super model, but this model still suffered from the limitations of linear elastic modeling, such as difficulty dealing with creep in concrete. The creep effect makes concrete respond more like a viscous fluid than an elastic solid in very particular conditions and unless the model is capable of applying the different properties selectively as appropriate to the situation, one set of properties must be applied throughout the model, which leads to non-physical material properties being used.*

In response to these limitations, PII *developed a Global Visco-elastic Abaqus model that selectively applies the appropriate creep response for the local conditions. The result is appropriate calculation of delamination with realistic material parameters and radial displacements that agree well with benchmark data. The model uses the Lee-Fenves concrete damaged plasticity properties (ibid.). The model includes individual tendons and specifically models the steel properties of the liner, conduits, and rebar... The Abaqus global model is run using the sparse solver in Abaqus/Standard and the various sub-models are run in both Abaqus/Standard*

and Abaqus/Explicit. The global model provides displacement data to the edges of the panel sub-models and other sub-models, which further provide higher resolution of localized behavior. The driven sub-models include stress models and concrete damaged plasticity models, all within Abaqus.

Each and every curved tendon in the containment was explicitly modeled using embedded beam elements in the global model. The tendons were assigned the cross-sectional stiffness of the sleeves and loads were applied.

Partitions are included in the structure to allow for the selective removal of concrete in the SGR opening, in the SGR delamination crack region, in the excavation regions of bay 34, and at the openings of the equipment and personnel hatches. Rebar is included in both the global and sub-models. This is implemented using the `*REBAR` capability within Abaqus, which entails converting all of the host elements to solid continuum shell elements with stack directions (sweep directions) oriented radially. Sleeve and tendon host elements remain as solid continuum elements and rebar host elements are implemented using continuum shell formulation.

Modeling of all tendons individually in both the global mesh and he sub-models, they could be individually loaded.

Long term visco-elastic creep is calculated by the Abaqus solver Creep is calculated from the actual stress state after design-load tensioning, which accounts for local variations in the stress, rather than by applying an approximation such as a global average shrinkage strain.

The global displacements, stress state, creep law, and the concrete damaged plasticity parameters are all implemented into the sub-models. This results in two technical barriers: Abaqus does not normally allow both mapping of the stress state and sub-modeling to be used simultaneously; and, Abaqus does not normally allow the creep law and the concrete damaged plasticity parameters to be used simultaneously. In order to overcome these hurdles: **redacted** lines.

The Abaqus Global model has four sections in the containment wall: a steel liner plate, an inner concrete cylinder, a hoop tendon sleeve layer, and an outer concrete cylinder. Curved sections of tendon sleeves are matched to the mesh. The average value of tensile stress is about 23 psi. It increases to 31 psi due to concrete displacement.

Until recently the resolution was to adjust the tensile capacity of the concrete to compensate for this. That is why a capacity of **redacted** *psi was assumed in global calculations. It does not affect radial displacement but it does facilitate the delamination evaluation. With the creation of the detailed sub-model the peak stresses become more visible and a tensile capacity of becomes appropriate. Note that even at a* **redacted** *inch mesh size there is still significant averaging of peak stresses occurring.* **redacted lines**

Recent analysis shows marginal improvement going from a **redacted** *such that the underestimation of peak stress by about* **redacted**.

Applying that factor to the assumed tensile capacity of **redacted** *for an infinitely small mesh. That corresponds to the measured tensile capacity of CR-3 concrete. The average direct tensile capacity measured in 9 samples was 448 ± 73 psi. The average split tensile capacity measured in 10 samples was 594 ± 59 psi and it is generally accepted that tensile capacity is 90% of the tested split tensile capacity. That gives 535 psi. Fracture energy is similarly impacted.*

There are a number of ways to address the mesh issue. For radial displacements or general stress calculations, **redacted** *mesh is sufficient to obtain realistic values. For scenarios which depend heavily on peak stress values one approach is to use a stress concentration factor. Recent comparisons indicate that for global Abaqus that factor would be about* **redacted**. *For the detailed sub-model it would be about* **redacted**. *Another way to achieve exactly the same result is to adjust the tensile capacity of the concrete. For events such as the onset of delamination, the details of the process are very sensitive to the peak stresses involved and fine mesh analysis is the best approach. Once initiated, delamination is less sensitive to peak parameters so the overall extent and width of cracking can be well described by a detailed sub-model or even the normal sub-model.* **redacted lines** in the report.

Global Model The report identifies the global model as composed of the following subparts:

Liner *Thick conventional shell elements with elements located on the inner surface of the concrete.* Fig. 8(a).

Inner Cylinder: which goess from the liner 29" inside, that is to the outer edge of the vertical sleeves. It is modeled by *two layers of continuum shell elements each with 5 integration point through the thickness for bending accuracy.* Fig. 8(b).

Hoop Conduits: *all hoop conduits are explicitly modeled as beams with pipe sections. Only curved sections are modeled on which a radial line load is applied.* Fig. 8(c).

Hoop Layer is a 5.25" thick layer which encompasses th vertical and horizontal sleeves. It is modelled by *solid elements with damaged plasticity material property based on the Lee-Fenves model (Lee and Fenves, 1998). These regions are allowed to crack and potentially to delaminate. The green regions are not allowed to crack since those regions are reinforced with steel.* Fig. 8(d).

Outer Cylinder: a 7.125" layer of concrete from the edge of the horizontal sleeves to the outer concrete, modeled by *one layer of continuum shell elements with 5 integration points for accurate bending representation.* Fig. 8(e).

Damage Material Regions *regions of the hoop layer which has the concrete damage plasticity material properties. These regions are allowed to crack and may result in delamination of the outer cylinder from the inner cylinder.* Fig. 8(f).

Driven Regions: *The region is driven by the displacements form the global model. The displacements are synchronized with the loadings in the delamination model. Hence, the global effects due to tensioning, creep, and SGR detensioning (including the unloading of the 10 vertical tendons) are accounted for.*, Fig. 8(g).

(a) Liner (b) Inner Cylinder (c) Hoop Conduits (d) Hoop Layers (e) Outer Cylinder (f) Damage Material Regions (g) Driven Regions

Figure 8: Group 7 Finite element analyses; global sub-model (ADAMS Accession No. ML 102861026, 2010)

Detailed Model The detailed model included 6 horizontal and 3 vertical tendons as shown in Fig. 9. Radially, it matches the global mesh for ease of boundary condition transfers. Again, contrarily to the global one, the inner cylinder is modeled by a nonlinear constitutive relationship, and it is analysed by the explicit version of Abaqus.

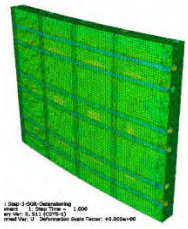

Figure 9: Detailed model (ADAMS Accession No. ML 102861026, 2010)

2.2 Computer Model Validation

Early in this section PII refers to the validation of the model: *Because benchmarking is an important validation technique, the codes used in this computer analyses were benchmarked against the known plant response to the Structural Integrity Test performed in 1976. In addition, the computer model predictions were compared with containment interior laser scanning performed in March, 2010 during the de-tensioning that was done prior to repair bay 34.*

Benchmarking results was preceded by the same comments as in Sect. 2.1 with regard to Abaqus, NASTRAN and material properties. Results, with the 1976 Structural/System Integrity Test (SIT) is shown in Fig. 10, and those with the interior laser scanning performed in 2010 during detensioning in Fig. 11. It should be noted that laser scanning was performed after each group of tendons (referred to as a Pass) was de-tensioned from after Pass 4 until after Pass 11. Pass 4 was taken as the baseline for all the readings so the Pass 11 data represents the change in radial displacement from Pass 4 through Pass 11.

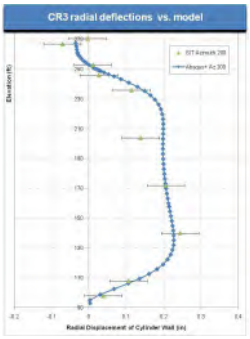

Figure 10: Comparison of measured radial deflections during the 1976 CR3 SIT taken at azimuth 200 degrees (Az 200) with PII computer model predictions (ADAMS Accession No. ML 102861026, 2010)

2.3 Failure Modes in Group 1: Containment Design

In this first set of reported analysis, PII alleges that high stress concentrations played a partial (but not decisive) role in the delamination.

Some of the relevant quotes include:

1. *FM 1.1 determines that CR3's containment design results in high vertical and hoop compression stresses and radial tensile stresses when compared to the designs of other plants. FM 1.15 determines that stress concentration factors (SCFs) were not explicitly considered in the original design of the containment building. FM 1.2 determines that radial stresses in the containment structure are high and that no radial reinforcement is currently in place. As with all the confirmed Failure Modes, the conclusions reached indicate that these issues did not individually cause the delamination, but rather contributed to the conditions that resulted in delamination.*

2. *The large diameter tendons have another impact as well. They are located at a depth of 10 inches from the outer containment wall with a set of tendons about every 39 inches. At that depth 27% of the cross-sectional area has the concrete displaced by tendon sleeves.*

3. *A horizontal tendon provides the radial compressive stress of about 340 psi averaged over the diameter of the tendon sleeve. The average over the entire cross-section of concrete being radially compressed by that horizontal tendon is about 100 psi. Normally the average radial tensile stress would be 23 psi but due to concrete displacement it is 31 psi at the centerline of the horizontal tendons.*

The analysis used to support this finding is also reported later on in conjunction with the Group 2 analysis.

To support the allegation, PII reports *not to use NASTRAN to quantify concrete fracture so fracture parameters are not applicable. Abaqus applies creep correction only for long time period intervals such as the time step of 30 years of operation with the containment tensioned. E0 is the elasticity modulus and E1 is the*

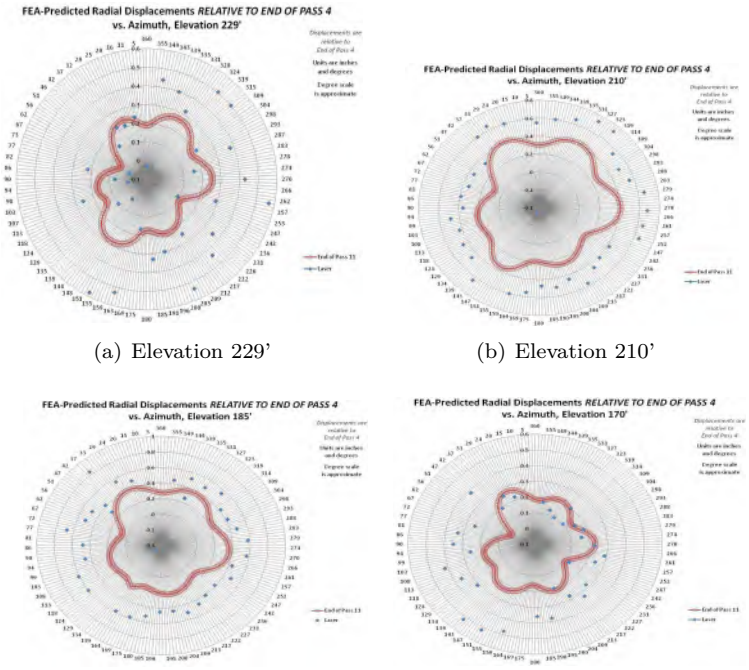

(a) Elevation 229' (b) Elevation 210'

(c) Elevation 185' (d) Elevation 170'

Figure 11: Comparison of PII computer model predictions for radial displacement from pass 4 through pass 11 at various elevations to the laser scanning data (ADAMS Accession No. ML 102861026, 2010)

creep adjusted elasticity modulus. F't is tensile capacity and G't is the fracture energy. 3.45$\times 10^6$ *psi is the average modulus measured on 22 CR3 containment cores. Fracture energy was measured to be 0.40 lbf/in.* A "measured" fracture energy of 0.40 lbf/in is used, and the material properties of Table 2 are reported.

Figure	Model	E_0	E_1	$f't$	G'_t	Creep
12(a)	Abaqus Detail	3.45×10^6	3.45×10^6	360	0.08	2.2
12(b)	Abaqus Detail	3.45×10^6	3.45×10^6	360	0.08	2.2
12(c)	Nastran	4.29×10^6	4.29×10^6	NA	NA	o

Table 2: Material propertis for Group 1 Analyses

On the basis of Fig. 12(a), PII points to the *peak tensile stress at the edge of the horizontal tendon hole near a vertical tendon is well in excess of the tensile capacity of the CR3 concrete. It is likely that small cracks formed at these intersections but then stopped propagating when they reached a location where the stress was too low to continue.*. This is further illustrated by Fig. 12(c).

PII concludes that:

FM 1.1 *determines that CR3's containment design results in a somewhat higher potential for delamination than other similar designs on the basis of Compressive-Tensile Stress Interaction*

FM 1.2 *finds that radial tensile stresses are high and there is no radial reinforcement. Large tendons lead to high peak stresses.*

FM 1.15 *identified that stress concentration factors were not explicitly considered in the original design of the containment building. As with all the confirmed failure modes, they conclude that these issues did not individually cause the delamination but contributed to the conditions that resulted in delamination.*

Considered alone, the stresses involved in the CR-3 containment design are well within the capability of the concrete material used. However, when stresses occur for other reasons, such as local stresses resulting from

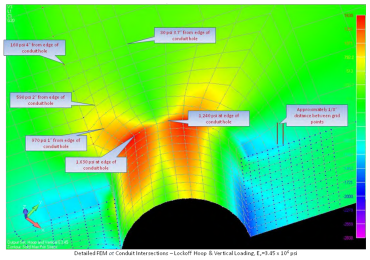

(a) Stress contours for normally tensioned conditions at the intersection of a vertical and horizontal tendon.(3 Dimensional Effect Looking Through a Hoop Tendon Hole)

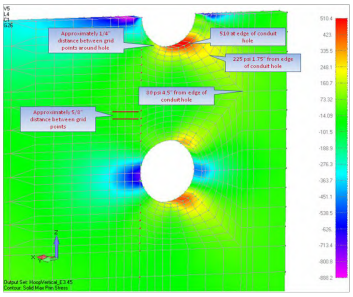

(b) Sketch of the delamination cracking in the bay 34 wall.

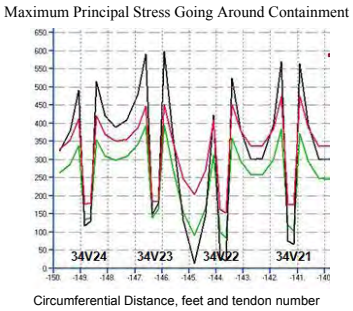

(c) Plot of maximum principal stress as a function of distance around the containment circumference. (Black is pre-SGR, Green is Post SGR de-tensioning, Red is post SGR concrete removal).

Figure 12: Group 1 Finite element Analyses (ADAMS Accession No. ML 102861026, 2010)

de-tensioning of tendons and cutting the opening, these additional stresses at CR3 contribute to the overall stress condition.

2.4 Failure Modes in Group 7: SGR Activities

This second group addresses *s FM 7.3/7.4 Inadequate de-tensioning sequence and scope; and FM 7.5 Added stress due to removing concrete at the opening*[3]

The computer model and its validation were presented in attachements 1 and 2 in the report. However for increased clarity, and given their importance, they were presented above in this one.

Discussions The report starts by discussing the inadequacy of the de-tensioning sequence and the *added stress due to removing concrete at the opening.* It points out the impact of a change from a symmetric load and deformation to an unsymmetric one on *stresses and strains that may exceed its capacity.* Also mentioned is the potential for *excessive stresses and/or strains can develop when transitioning between two symmetric states because of the sharp local transition from a series of tensioned tendons and a series of de-tensioned tendons..* Reference is made to Fig. 14(d) which *shows the radial displacement that occurred during the SGR de-tensioning. Delamination occurs where radial stress is high. That occurs at sharp bends in the wall... Note in Figure 14(d) that the radial displacement associated with de-tensioning is linear. This means that the stress that develops is monotonically increasing and other sequences of de-tensioning the same number of tendons would not change the end-point which is the highest stress condition.*

The report does also mention that *In an area as large as bay 34 and with the large stress concentration factors on a detailed scale, it is probable that cracking began in isolated points of highest stress. As the stresses increased (due to the growing number of de-tensioned tendons), and shifted (due to the various tendons de-tensioned), small cracks grew and joined until they eventually covered the entire delaminated area.*

it is clear from the finite element analysis that the localized de-tensioning in bay 34 led to curvature which contributed to the delamination. The March, 2010 analysis and subsequent de-tensioning for repair found that use of more symmetrical de-tensioning of the entire circumference was required to avoid delamination in other bays and the building was successfully de-tensioned.

[3]Presentation of the failure modes associated with this group was deemed to be very convoluted by the author. As such, headings and order of coverage were modified, but the content strictly adheres to what the report has presented. No comments were interjected, these will be presented later in Sect. 3.

Global Radial Response Tendon de-tensioning simulation, using the previously described model, was simplified by not *relaxing the tendons in order but, instead, relaxing all the tendons partially at the same time. Thus 25% through the de-tensioning means all tendons are stressed to 75% of their lock-off value.*

The Sequence was as follows:

1. *The containment is initially constructed with straight vertical walls. Radial displacement is 0 inches since this is the measurement baseline, Fig. 13(a).*
2. *Upon completion of tendon tensioning the building is mostly symmetrical and each bay has an inwardly curved wall with a maximum deflection of -0.5 inch, Fig. 13(b).*
3. *Over the next three decades the concrete creeps and radial displacement grows to a maximum of -1", Fig. 13(c).*
4. *As SGR de-tensioning proceeds, bay 34 begins to move radially outward. Bays 23 and 45 also begin to move radially outward at half the rate of bay 34 because bay 34 has shared tendons with each of bays 23 and 45. The other bays begin to move inward in response to the buttresses having unbalanced side loads. The building develops an overall vertical curvature Fig. 13(d).*

Figure	Model	E_0 psi	E_1 psi	f'_t psi	G'_t lbf/in	Creep
13(a), 13(b), 13(d), 13(e), 13(f), 14(a), 14(c)	Abaqus Global	3.45×10^6	3.45×10^6	NA	NA	2.2
14(e), 14(f) 12(b),	Abaqus Global Bay sub model	3.45×10^6	3.45×10^6	108	0.08	2.2
13(c), 14(b), 14(d)	Abaqus Global	3.45×10^6	1.1×10^6	NA	NA	2.2
12(b), 17(a), 17(b), 17(c), 18	Abaqus Global Bay sub model	3.45×10^6	3.45×10^6	360	0.08	2.2

Table 3: Material properties used in the detnsioning simulations

The global response of the container in terms of displacement is captured by *Figures 13(a) to 13(d)* [that] *show the progression of containment shape over time. It was originally a cylinder but it became concave with the tensioning of the tendons. The SGR de-tensioning sequence resulted in a building-wide change in shape and bay 34 moved out close to its original tensioned position prior to creep, Fig. 14(d).* The report does

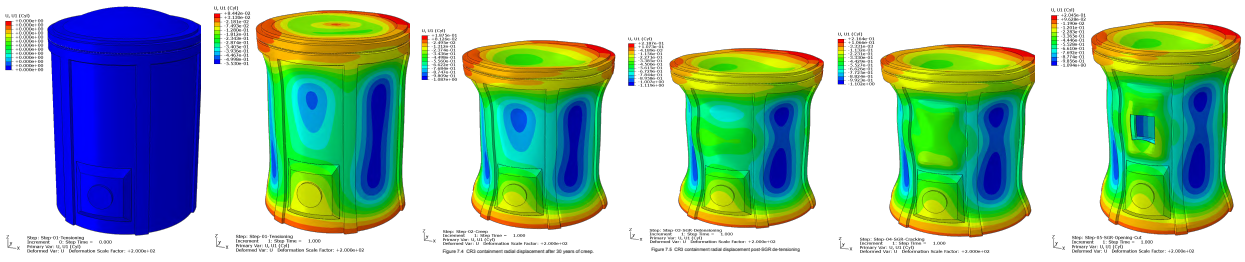

(a) Untensioned (b) Fully tensioned (c) After 30 years of creep (d) Post SGR de-tensioning (e) Post SGR de-tensioning (f) After SGR opening completion

Figure 13: CR-3 Containment radial displacements (ADAMS Accession No. ML 102861026, 2010)

provide qualitative support for the observed radial displacement.

Delamination Explained To explain the observed delamination, focus is then placed on the details of the local wall-radial displacement response based on the global model first and then on the detailed one.

The following statement is offered for *The report will be providing some computer model plots which had the following inputs that were used based upon testing and modeling. PII does not use NASTRAN to quantify concrete fracture so fracture parameters are not applicable. Abaqus applies creep correction only for*

long time period intervals such as the timestep of 30 years of operation with the containment tensioned. E_0 is the elasticity modulus and E_1 is the creep adjusted elasticity modulus. f'_t is tensile capacity and G'_t is the fracture energy. 3.45 $\times 10^6$ psi is the average modulus measured on 22 CR3 containment cores. Fracture energy was measured to be 0.40 lbf/in. Abaqus Global does not calculate fracture so those parameters are Not Applicable for it.

Global Model Using the model previously described, the report prurport that it was indeed capable of capturing the field observed delamination from the global model.

Figs. 14(a) to 14(c) show the (displacement) contour lines of the global model (subjected to a linear elastic analysis) at various stages. Fig. 14(d) is a plot of bay 34 midline profile at various stages. Delamination is observed in Fig. 14(e) and 14(f) right before concrete removal and after concrete removal. Displacement contour lines in Fig 14(e) is compared to the field observed extent of cracking shown in Fig. 15.

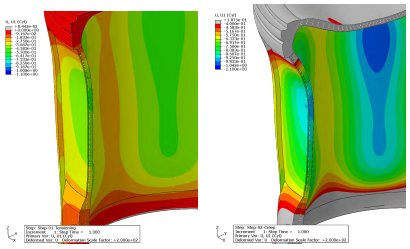

(a) Post initial tensioning in 1975 (b) After 30 years of creep

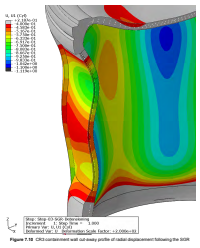

(c) After the SGR

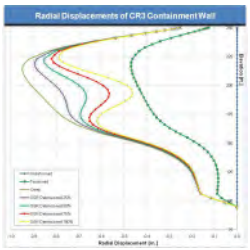

(d) Bay 34 midline profile for progressive SGR detensioning

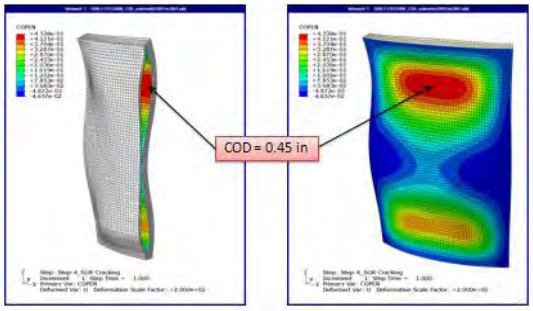

(e) Step 4

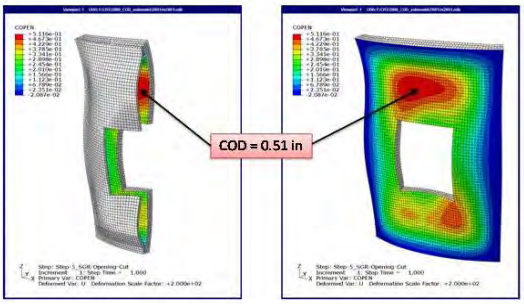

(f) Step 5 (after concrete removal)

Figure 14: CR-3 bay 34, cracking and crack opening displacement (ADAMS Accession No. ML 102861026, 2010)

Local stresses increased since the rest of the bay was still restrained by tensioned tendons, Figs. 16(a) to 16(h).

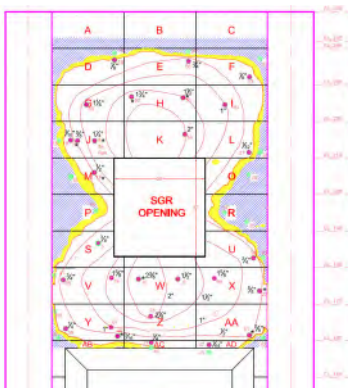

Figure 15: Plot of delamination damage in Bay 34. Shown are the measurements of the delamination gap both by impulse response test and by core bores.

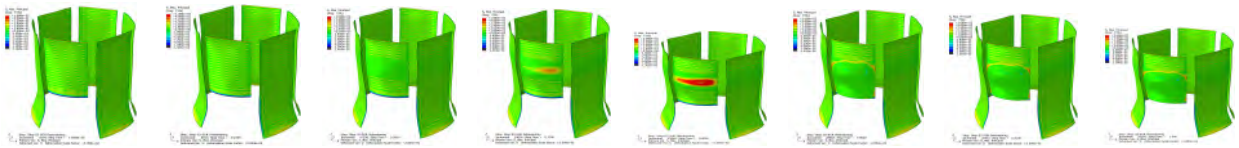

(a) Step 1/20 (b) Step 5/20 (c) Step 10/20 (d) Step 15/20 (e) Step 16/20 (f) Step 18/20 (g) Step 19/20 (h) Step 20/20

Figure 16: Maximum principal stresses (psi) (ADAMS Accession No. ML 102861026, 2010)

Detailed Model It is also shown that the detailed model was also able of capturing the delamination. This is observed in the panel and *the situation ultimately led to localized cracking that propagated over most of bay 34, Fig. 17(a) and 17(c)* The maximum stresses in the delaminated area are shown separately in Fig.

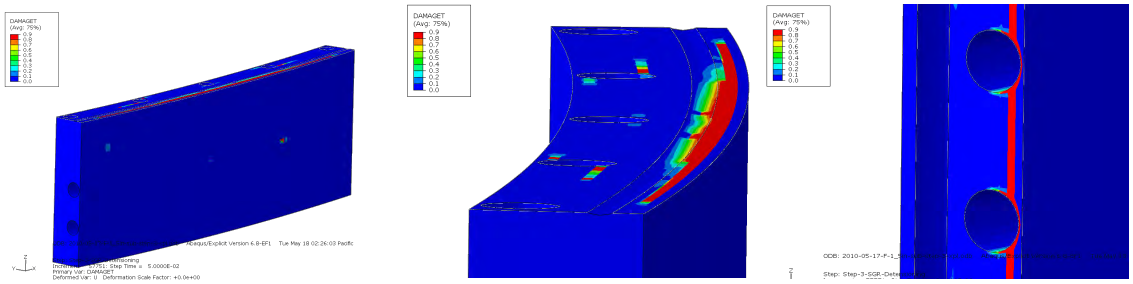

(a) Bay 34 wall segment approaching delamination (b) Bay 34 wall segment delaminating (c) f_t'= 360 psi

Figure 17: Bay 34 wall segment delamination

18.

3 Critical Review

Undoubtedly, a very detailed (numerical) investigation was performed. There was a recognition of the complexity of the problem, and as a result advanced nonlinear analyses were performed. However, we found the report difficult to follow (and not only for the many redacted portions).

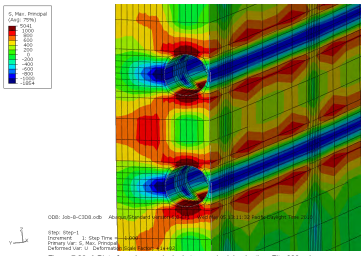

Figure 18: Plot of maximum principal stresses in delamination. f'_t =360 psi. (ADAMS Accession No. ML 102861026, 2010)

3.1 Analysts/Analysis

ADAMS Accession No. ML 102861026 (2010) provides the *curriculum vitae* of those involved in the reported analysis. Surprisingly, none of them seem to have any experience in the analysis of reinforced concrete, let alone in nonlinear analysis. Having experience with a tool such as Abaqus for mechanical design, does not qualify someone to perform the investigation of a multi-million dollar accident. Regretfully, this lack of expertise transpires throughout the report where technical terms are often misused, repeated, out of context; confusion seems to prevail, and results highly questionable. For example on page 32 "Abaqus Global does not calculate fracture so those parameters are not Applicable for it" Abaqus is not supposed to calculate fracture, there is nothing to calculate, Abaqus is supposed to capture or localize fracture. Why is then $G't$ associated with Abaqus global analyses.

3.2 Validation

"Benchmarking" of the code results are inconclusive at best. SIT (in theory) should not have induced any nonlinearity (cracking or otherwise), hence excellent correlation between measurements and computations should be expected. Indeed adequate correlation is reported, however this does not necessarily validate the code for nonlinear analyses.

Validation with the 2010 detensioning is inconclusive as there are too many variations in laser readings, and errors bars are not included for either of the two reported values (experimental or numerical). The term "Benchmarking" is unfortunate, a more traditional term would have been "Validation" or possibly "Calibration" (as it is reported later that elastic properties have been modified to yield adequate correlation between numerical findings and field observations).

The nonlinear constitutive model used for the detailed model (Lee and Fenves, 1998) is far from simple. Some of the key input parameters include

$\overline{D}_c$, $\overline{D}_t$	Measured elastic stiffness degradation for uniaxial compression and tension respectively.
G_c G_t	Compressive and tensile fracture energies respectively.
l_c, l_t	Compressive and tensile characteristic length parameters respectively.
α, β	Coefficients of the yield function.

Except for G_t, none of the other parameters are provided. Hence, one can easily fine-tune the model to obtain desired results but such an approach is highly circumspect The selected parameter should have been first validated independently, and then tabulated in the report (as they were in the original paper by Lee and Fenves).

3.3 Elastic Modulus and Visco-Elasticity

The report addresses the finite element model used for group 1. We find it confusing. The authors start by professing not to use NASTRAN to quantify fracture, and as such fracture parameters are not applicable. Yet ever since the pioneering work of Hillerborg, Modéer, and Petersson (1976) any modern investigation of concrete fracture would have to use fracture mechanics. The website of the International Association

of Fracture Mechanics of Concrete and Concrete Structures (IA-FraMCoS), with over a thousand indexed papers, is a testimony of the rich and relevant literature associated to the fracture mechanics of concrete.

In the document, reference to creep is made in conjunction with $G't$ the fracture energy. It is assumed that the authors meant $G'F$ which is the concrete fracture energy, and is completely unrelated to creep[4]. Furthermore the table entry labeled "Creep" may be misleading, it is assumed that the authors meant "Creep Coefficient".

A particularly troublesome approach taken by the authors is the liberty with which material properties are at times modified to match intended results. In the table, E_0 is equal to 3.45×10^6 in the Abaqus analyses, and 4.29 in the NATRAN analyses, Table 2.

The global model used is labeled visco-elastic fracture. Yet there is no fracture modeled whatsoever, and visco-elasticity is a term usually reserved for those models where creep and linear response are separable (that is the model is expressed by a relaxation function). In the reported analysis, the so-called visco-elasticity (which Abaqus has implemented) is instead modeled by reducing the elastic modulus through the creep coefficient.

Whereas the reported assumed value of $E = 1.1 \times 10^6$ psi *allowed the model to predict the onset of delamination* [with] *significant uncertainty* it is not clear how it correlates with he earlier reported value of 3.45×10^6 psi. It is not at all clear if this reported value of 1.1×10^6 psi is E_0 which will then be reduced by creep, or if it is the creep reduced value. Coincidentally, this value may be acceptable on the basis of an assumed creep coefficient of 2.2 (not supported by referenced laboratory tests)

$$E' = \frac{E}{1+\xi} = \frac{3.45 \times 10^6}{1+2.2} = 1.07 \times 10^6 \text{psi} \tag{2}$$

This coefficient is applicable in the absence of reinforcement which is known to drastically reduce creep. Indeed, Equation 9.5.2.5 of ACI 349 (2006) states *Unless values are obtained by a more comprehensive analysis, additional long term deflection resulting from creep and shrinkage of flexural members shall be determined by multiplying the immediate deflection caused by the sustained load considered by the factor* λ_Δ

$$\lambda_\Delta = \frac{\xi}{1+50\rho'} \tag{3}$$

where ρ' *shall be the value at midspan for simple and continuous spans.... It shall be permitted to assume* ξ*, the time dependent factor for sustained loads, to be equal to 2.0 for 5 years or more.* A commonly accepted reinforcement ration for a NCS can vary from 0.5 to 1%, thus

$$\lambda_\Delta = \frac{\xi}{1+50\rho'} = \frac{2.}{1+50\times[0.005|0.01]} = [2.3|1.98] \tag{4}$$

These values correspond to the reported one used in Eq. 2 but unfortunately, the document is not at all clear which E is used. The finally selected values are blacked out.

3.4 Tensile Strength

There is a "mystery" surrounding the actual value of the tensile strength used with references to "adjusting its value".Many of the critical information, of what should be a laboratory measured value, are redacted.

3.5 Modeling

To better understand and visualize the model adopted by PII, Fig. 19 was prepared by the author. Further explanation is provided later.

Point loads in the Sleeves Tendon loads in the sleeves were applied as line loads. This induced a stress singularity which may have been interpreted as cracking. This is clearly visible in both Fig. 12(a) and 18. Those are "distractions" from the actual stress field which may have caused cracking/delamination. Modeling the stiffness of the sleeve is very unlikely ot have sufficiently smoothened or distributed the point load into a traction wide enough to avoid stress singularity.

Finally, the reader should consult (Acharya and Menon, 2003) for a good coverage of this delicate topic.

[4]Disclaimer: The fracture energy tests were performed under contract from PII by the author.

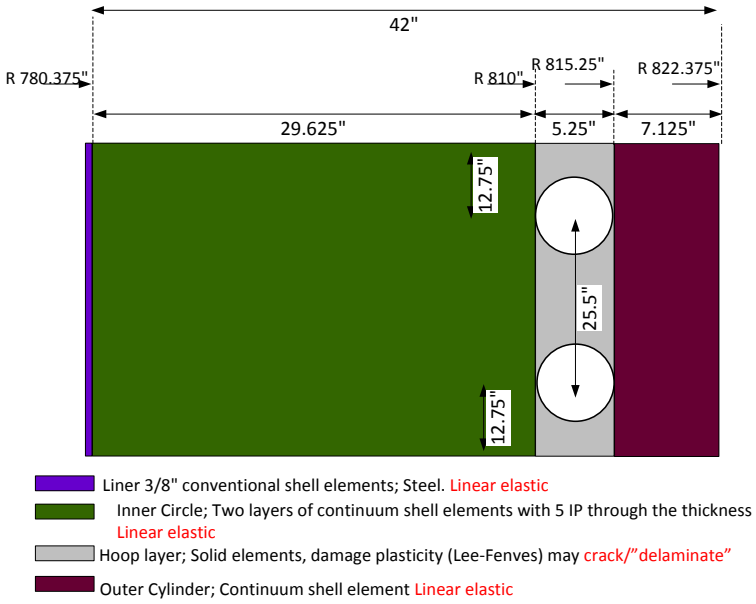

(a) PII global & refined model

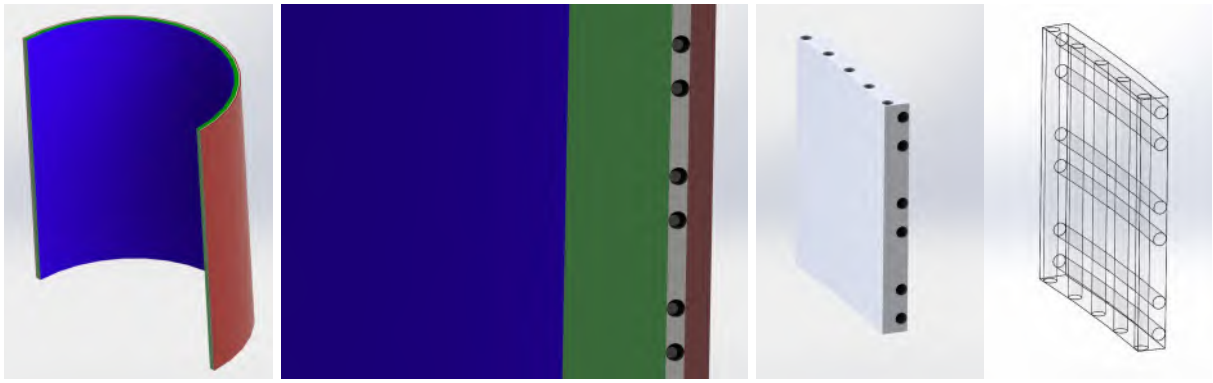

(b) Global model (c) Closeup of global model (d) Refined model

Figure 19: Models

Reinforcements In a structure as complex as CR-3, clearly there are zones with heavier reinforcement than others (around the hatch for instance). Yet the reinforcement modeling is not explicitly addressed. It is not expected that reinforcement should be modeled explicitly, but as a minimum the elastic properties of concrete should be replaced by an "weighted modulus" based on the reinforcement ratio ρ

$$E_{eq} = E_c + \rho_s E_s \tag{5}$$

From Global to Detailed A two tier analysis for complex structures is not unusual (this is commonly referred as "substructuring" in finite element parlance). it is not clear how the boundary conditions are transferred from the global to the detailed model, specially that the report mentions a so-called "driven region" Fig. 8(g) Finally, the panel (detailed model) should be subjected to high vertical compressive forces caused not only by the post-tensioning but also the self weight of the structure. There is no indication that this was accounted for.

How is it all put together? This is possibly the major concern for this author:

1. There is no indication in the report on how the various constituents of the global or detailed models are connected. Is there a full connection, are nodes master-slaved, or are they assumed to act independently as a parallel system (as opposed to a single one)?

2. In the absence of such information, and in view of the observed "delamination" (Fig. 14(e), 14(f) and 8), indications are thee constituents were not all tied together, and as such, of course a "delamination" will be observed. As discussed in the next section, the analyst should have tied the damage material region, Fig. 8(f) to the adjacent ones by joint/interface zero-thickness elements commonly found in most finite element codes. These can range from the simplest ones (Goodman, R.E. and Taylor, R.C. and Brekke, T.C., 1968) to the more advanced fracture mechanics based one (Cervenka, Chandra, and Saouma, 1998).

Keeping in mind that there is a one way coupling (that is from global to the detailed model) and that the simplified linear elastic global model was able to capture delamination (Fig. 14(e), 14(f)) why was there a need to perform the detailed analysis and then capture the delamination in Fig. 8?

the delamination in the global model is captured as a separation of nodes (implying that no interface elements were used), and in the detailed model, is conjunctured that it occurred in light of the damage zone showed through the continuum elements in Fig. 8.

Explicit Analysis An explicit model will always yield some result. However, because equilibrium is not checked at the end of each increment, one has to be extremely careful in accepting the results of such an analysis. Indeed the Lee and Fenves (1998) model adopted is known to be extremely unstable in implicit analysis, but will always yield results in an explicit one. A palliative to this concern is to ensure balance of energy throughout the analysis.

Weak and Strong links There is an imbalance in modeling effort. On the one hand "strong links" are present in modeling the sleeves of the tendons which is not needed, neither one would have needed to have such a fine mesh. On the other hand, there are "weak links" as the reinforcement does not seem to be modeled, and the various components of the mesh were not "glued" together.

4 Alternative Analysis by the Author

Based on (ADAMS Accession No. ML 102861026, 2010) and (Progress Energy Florida (ML102861026), 2009) a renewed analysis of CR was undertaken by the author.

4.1 Assumptions and Model

Finite element modeling of Crystal River containment structure, detensioning sequence, staged "excavation" of the concrete cover, and finally ensuing delamination is a challenging task. Ultimately, a finite element model is an engineering compromise between accuracy, representativeness, simplicity, elegance, computational cost and most importantly good understanding of the physics governing the problem being solved. In this case, given that delamination is a manifestation of cracking, the solution has to be rooted in fracture mechanics, as after all one is trying to capture cracking of a brittle material, and plasticity is of little relevance in this case.

A particularity of this analysis, is that the crack trajectory is known as it is a (curvilinear) plane connecting the sleeves where delamination occurred. As there is no indication that concrete crushed as a result of compressive stresses exceeding approximately half the compressive strength, all the nonlinearity would stem from cracking. As such, a discrete/cohesive crack model (Červenka, J., 1994) (Cervenka, Chandra, and Saouma, 1998) would better capture it than a smeared (diffuse) crack one. In CR, delamination occurred (in the duct plane) in an unreinforced direction, (gray zone in Fig. 20(a)).

Accordingly, a suitable model is one that:

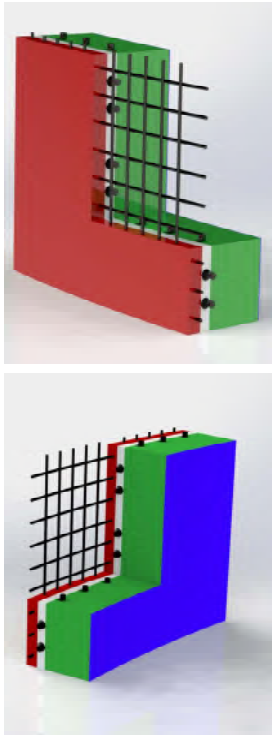

(a) Cut rhough conceptual model (viewed from extrados and intrados)

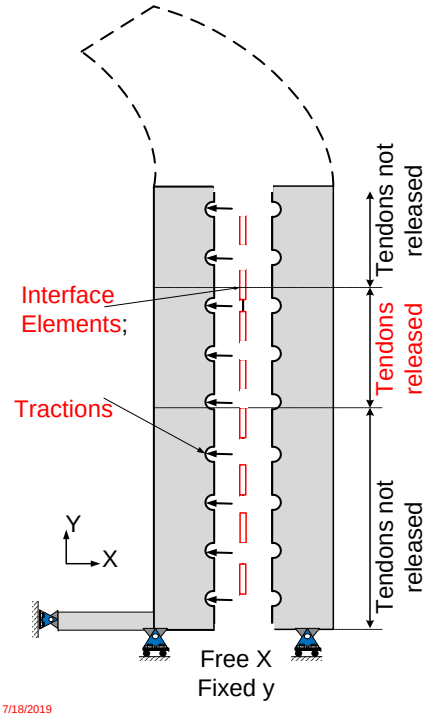

(b) Structural idealization for finite element mode

Figure 20: CR Idealization

- Takes advantage of geometrical symmetry (180°), Fig. 21(a). Though, it should be noted that post-tensioning cable layouts violate it, however this was a reasonable compromise to ensure reasonable computational cost.
- Restricts the nonlinearity (i.e. cracking) to the delamination plane.
- Sleeves holes are individually modeled, and an inward traction models the hoop post-tensioning (which are ungrouted) as individual radial forces, Fig. 20(b).
- Reinforcement is either smeared over the elements (reinforcement mat) or an effective elastic modulus (in terms of E_c and E_s) is adopted (around the batch).
- Models vertical prestressing as a set of point forces.
- Dome's prestressing is modeled as a uniform (downward) radial traction.

Hence, a total of 19 material groups were used, some had identical properties, but were separately defined in order to model the "peeling" of the concrete in the Steam Generator Replacement opening (SGRO), Fig. 21(b).

The load sequence leading to delamination is modeled in 17 increments, Table 4.

4.2 Results

Fig. 23(a) shows the global response (with highly amplified deformation) of the CEB, whereas closeups on the captured delamination are shown in Fig.23(b). We note the impact of the individual hoop tendons.

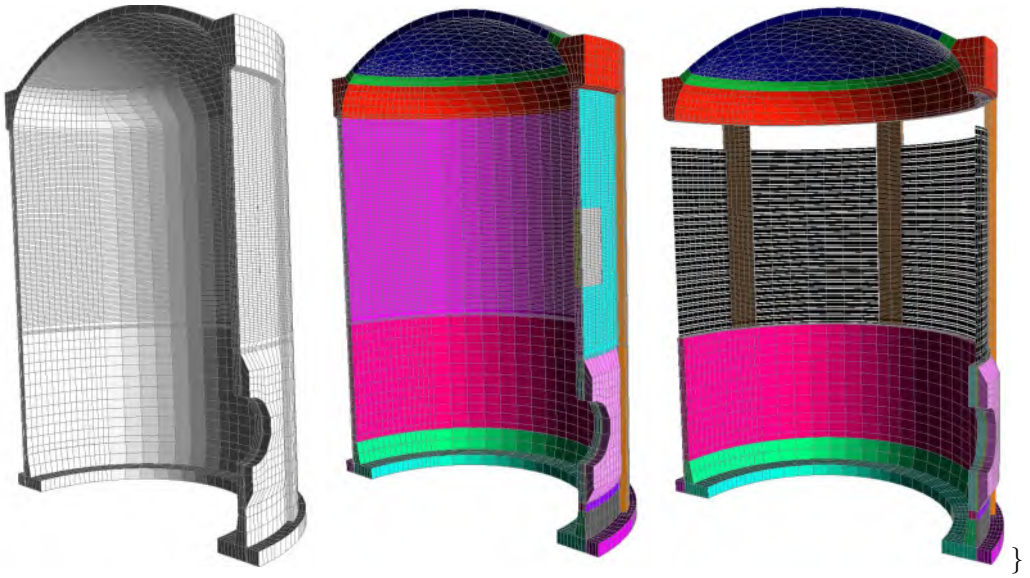

(a) Final final element mesh (b) Individual groups (c) Peeled concrete showing interface elements

Figure 21: Finite element mesh

Incr	Load	Incr.	Load
1	Gravity	2-3	Post-tensioning
4-5	Creep, Fig. 22	6-9	Cyclic temperature (inside/outside)
10-16	Cable detensioning in SGR zone	17	concrete removal (red layer in Fig. 20(a))
Delamination occurs			

Table 4: Load increment in CR analysis by authors

Though they have been detensioned, elastic recovery reduced the impact of the forces but creep recovery is still taking place (Fig. 22) and its impact clearly shown.

It is noteworthy that delamination was a brittle failure and not a progressive one. This is indeed characterstic of concrete shear/tension failure in the absence of reinforcement.

5 Conclusion

It is the author's opinion that delamination was caused by the abrupt change in curvature due to the detensioning of the cables inside the SGRO, i.e. not enough cables were detensioned as reported by Tampa Bay Times (2014). This could have been prevented should the tendons right outside the SGRO have been detensioned also in order to minimize abrupt curvature changes.

The simple, yet elegant, fracture mechanics based approach was capable of fully capturing the delamination of Crystal-River.

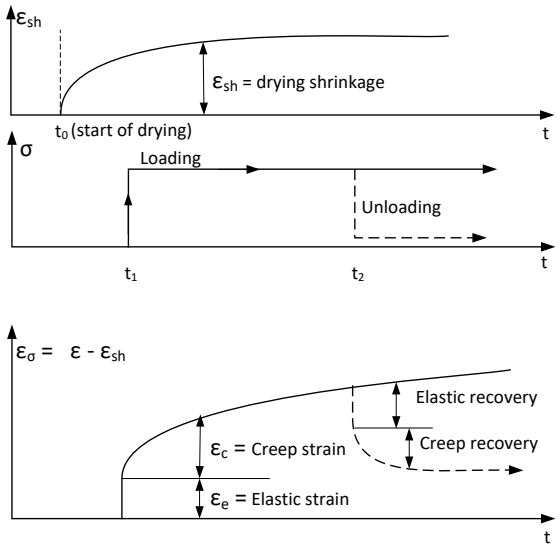

Figure 22: Role of creep

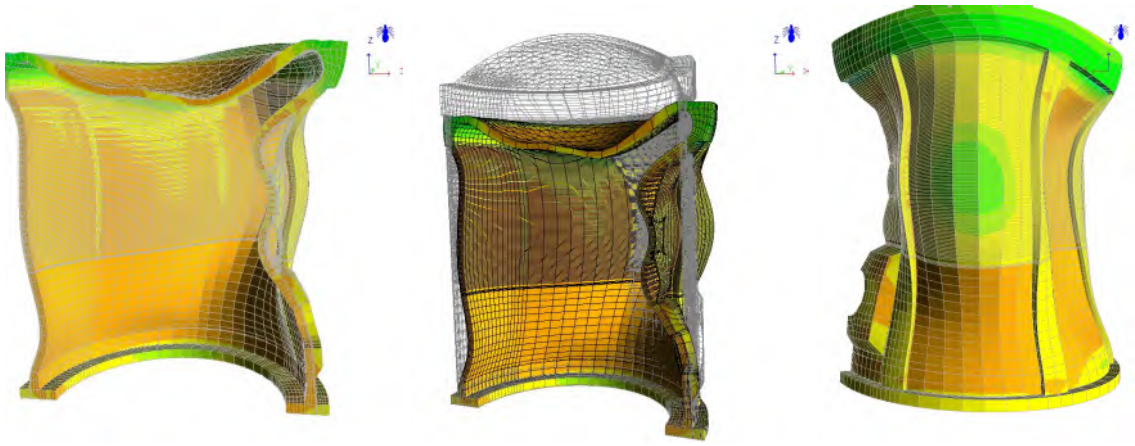

(a) Global response

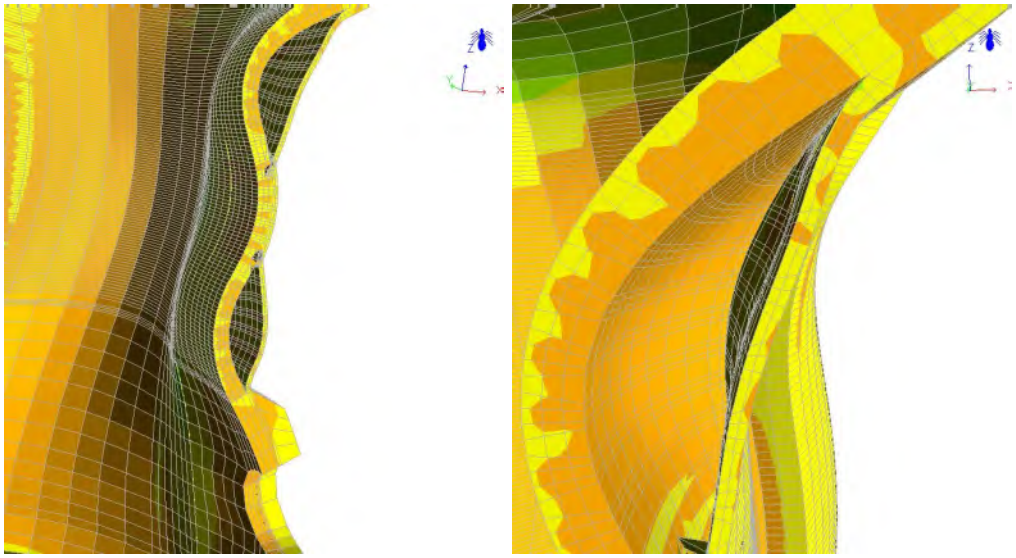

(b) Delamination details

Figure 23: Delamination of CR captured by a fracture mechanics based approach

References

Acharya, S. and D. Menon (2003). "Prediction of Radial Stresses due to Prestressing in PSC Shells". In: *Nuclear Engineering and Design* 225, pp. 109–125.

ACI 349 (2006). *Code Requirements for Nuclear Safety-Related Concrete Structures (ACI 349 M-06) and Commentary*. Tech. rep. American Concrete Institute, Farmington Hills.

ADAMS Accession No. ML 102861026 (2010). *Crystal River Nuclear Plant - Special Inspection Report 05000302/2009007*. Tech. rep. Nuclear Regulatory Commission.

Booker, Stephen et al. (1994). *Aging management guideline for commercial nuclear power plants-heat exchangers*. Tech. rep. Sandia Report SAND933-7070.

Cervenka, J., J.M. Chandra, and V. Saouma (1998). "Mixed Mode Fracture of Cementitious Bimaterial Interfaces; Part II: Numerical Simulation". In: *Engineering Fracture Mechanics* 60.1, pp. 95–107. DOI: 10.1016/S0013-7944(97)00094-5.

Chopra, O.K. (2015). *Effects of Thermal Aging and Neutron Irradiation on Crack Growth Rate and Fracture Toughness of Cast Stainless Steels and Austenitic Stainless Steel Welds*. Tech. rep. NUREG/CR-7185. U.S. Nuclear Regulatory Commission.

Goodman, R.E. and Taylor, R.C. and Brekke, T.C. (1968). "A Model for the Mechanics of Jointed Rocks". In: *J. of the Soil Mechanics and FOundations Division ASCE* 94, pp. 637–659.

Hillerborg, A., M. Modéer, and P.E. Petersson (1976). "Analysis of Crack Formation and Crack Growth in Concrete by Means of Fracture Mechanics and Finite Elements". In: *Cement and Concrete Research* 6.6, pp. 773–782.

Lee, J. and G. Fenves (1998). "Plastic-damage model for cyclic loading of concrete structures". In: *Journal of engineering mechanics* 124.8, pp. 892–900.

Los Angeles Times (2013). *How San Onofre's new steam generators sealed nuclear plant's fate*.

"NRC-ADAMS" (2018). *Agency wide Documents Access and Management System (ADAMS)*. Last accessed October 2018.

NuclearEnergy Insider (2019). *Crystal River to be decommissioned 50 years early*.

Progress Energy Florida (2011). *Petition To Determine The Reasonableness And Prudence Of Its Decisions On The Cr3 Steam Generator Replacement Project Leading Up To The October 2,2009 Delamination*.

Progress Energy Florida (ML102861026) (2009). *Crystal River Unit #3 Containment Delamination Update*. Accessed: July 2019.

Study of Post tensioning Methods (2015). Tech. rep. NUREG/CR-7208. U.S. Nuclear Regulatory Commission.

Tampa Bay Times (2014). *Settlement likely to end inquiries into Duke Energy nuclear plants*.

Červenka, J. (1994). "Discrete Crack Modeling in Concrete Structures". PhD thesis. University of Colorado, Boulder.